Preprints, 12th IFAC Workshop on Time Delay Systems
June 28-30, 2015. Ann Arbor, MI, USA

Pyragas-type feedback control for chatter mitigation in high-speed milling

N. van de Wouw [*,1] **N.J.M. van Dijk** [**] **H. Nijmeijer** [*]

[*] *Department Mechanical engineering, Eindhoven University of Technology, Eindhoven, Netherlands (e-mail: N.v.d.Wouw@tue.nl, h.nijmeijer@tue.nl)*
[**] *Philips Innovation Services, Eindhoven, Netherlands (e-mail: Niels.van.Dijk@philips.com)*

Abstract: Chatter is an instability phenomenon in high-speed milling that limits machining productivity by the induction of tool vibrations. In this paper, a design methodology for low-order Pyragas-type delayed feedback controllers is proposed. These controllers enable dedicated shaping of the chatter stability boundary such that working points of higher machining productivity become feasible while avoiding chatter. The control design problem is cast into a nonsmooth optimization problem, which is solved using bundle methods. Distinct benefits of this approach are the a priori fixing of the controller order, the limitation of the control action, and the fact that no finite-dimensional model approximations and online chatter estimation techniques are required. A representative example illustrates the merit of the proposed methodology in terms of increasing the chatter-free depth of cut, thereby enabling significant increases in the productivity of milling processes.

Keywords: Robust control, delay systems, high-speed milling

1. INTRODUCTION

High-speed milling is a widely used manufacturing technique to produce, for example, moulds and dies or components for the aerospace industry. The productivity in milling is often limited by the occurrence of an instability phenomenon called (regenerative) chatter. Chatter causes heavy vibrations of the tool resulting in rapid tool wear, an inferior workpiece surface quality, and noise.

The occurrence of chatter can be analyzed using so-called stability lobes diagrams (SLD). In an SLD, the chatter stability boundary between a stable cut (i.e. without chatter) and an unstable cut (i.e. with chatter) is depicted in terms of two key machining parameters: the spindle speed and depth of cut. To overcome chatter vibrations in high-speed milling and, therewith, to enable the chatter-free increase of the material removal rate, dedicated active control strategies are required.

Most of the results on active chatter control in milling involve the active damping of the machine dynamics (Dohner et al., 2004; Kern et al., 2006) or workpiece (Zhang and Sims, 2005). Damping the machine or workpiece dynamics, either passively or actively, results in a uniform increase of the stability boundary for all spindle speeds. To enable more dedicated shaping of the stability boundary (e.g. lifting the SLD locally around a specific spindle speed), the regenerative effect, which is inherent to the metal cutting process and which is the root cause for chatter, should be taken into account in chatter controller design (Shiraishi et al., 1991; Chen and Knospe, 2007; van Dijk et al., 2011a). All aforementioned research either does not include the regenerative effect during controller design or utilizes high-order finite-dimensional approximations of the milling model for controller design, yielding high-order controllers which is disadvantageous from an implementation perspective.

Building upon the results of (van Dijk et al., 2011b), this paper presents a *low-order* controller design methodology, which can guarantee chatter-free milling operations in an a priori defined range of process parameters, while explicitly taking into account the regenerative effect responsible for chatter. In particular, we propose a design for low-order chatter controllers for the milling process using Pyragas-type feedback (Pyragas, 1992). The choice for Pyragas-type feedback design is motivated as follows. An important aspect of the chatter controller design is the selection of the variable used for feedback, see (van Dijk et al., 2011a). In the latter paper, it has been shown that so-called perturbation feedback (i.e. only using the chatter vibrations, as opposed to the full vibration of the milling machine, in the feedback loop) is favorable in terms of limiting the control action, which is important in practice. To enable perturbation feedback, online estimation techniques for the chatter vibrations are needed since these cannot be measured directly, see (van Dijk et al., 2010, 2011a). Here, we propose an alternative way to achieve such perturbation feedback while still only using measurements of the full vibrations of the milling machine. To this end, we propose to employ Pyragas -type delayed output feedback, which avoids the need for complex online

[1] N. van de Wouw is also affiliated with the Department of Civil, Environmental & Geo- Engineering, University of Minnesota, Minneapolis, U.S.A., and with the Delft Center for Systems and Control, Delft University of Technology, Delft, Netherlands

estimation techniques for chatter vibrations by the grace of the structure of such type of control.

The main contributions of this paper are summarized below. Firstly, we propose a fixed-order controller design technique for the high-speed milling process. This technique guarantees the avoidance of chatter in a predefined range of working points (in terms of spindle speed and depth-of-cut). In this way, large increases in productivity (material removal rate) can be achieved while avoiding chatter. Secondly, the proposed control strategy has favorable properties from an implementation perspective in three ways. Firstly, it allows the user to prespecify the order of the controller and hence supports low-order controller design, which is desirable in a real-time implementation. Secondly, the proposed strategy limits the control action by employing so-called perturbation feedback and, thirdly, it implements such perturbation feedback through Pyragas-type delayed output-feedback. Additional contributions of the current paper with respect to (van Dijk et al., 2011b) are the following: firstly, the synthesis methodology has been extended to accommodate the design of *Pyragas-type delayed* output feedback control and, secondly, the inclusion of the design of *dynamic* output feedback chatter controllers (which can improve performance with respect to static controllers).

2. HIGH-SPEED MILLING PROCESS

A model of the milling process will be described concisely below, see e.g. (Altintas, 2000; Faassen et al., 2003; Stépán, 2001; Insperger et al., 2003) for more details.

In Figure 1, a schematic representation of the milling process is depicted. The predefined motion of the tool with respect to the workpiece is characterized in terms of the static chip thickness $h_{j,\mathsf{stat}}(t) = f_z \sin\phi_j(t)$, where f_z is the feed per tooth and $\phi_j(t)$ the rotation angle of the j-th tooth of the tool with respect to the y (normal) axis (see Figure 1). However, the total chip thickness $h_j(t)$ also depends on the interaction between the cutter and the workpiece. This interaction causes cutter vibrations resulting in a dynamic displacement $\underline{v}_t(t) = [v_{t,x}(t)\ v_{t,y}(t)]^T$ of the tool, see Figure 1, which is superimposed on the predefined tool motion and results in a wavy workpiece surface. The next tooth encounters

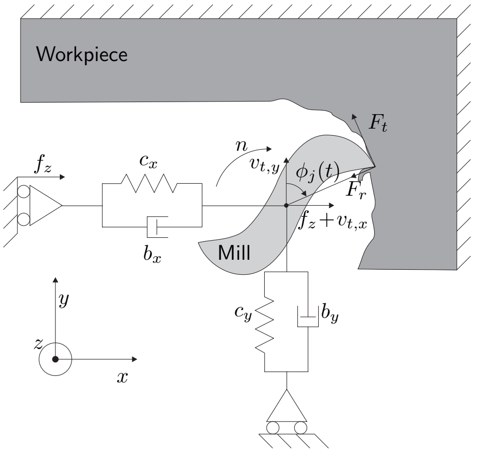

Fig. 1. Schematic representation of the milling process.

this wavy surface, generated by the previous tooth, and, in turn, generates its own waviness. This is called the regenerative effect. The difference between the current and previous wavy surface is called the dynamic chip thickness, denoted by $h_{j,\mathsf{dyn}}(t) = [\sin\phi_j(t)\cos\phi_j(t)]\,(\underline{v}_t(t) - \underline{v}_t(t-\tau))$ with $\tau = 60/(zn)$ the delay, z the number of teeth and n the spindle speed in revolutions per minute (rpm). Hence, the total chip thickness removed by tooth j at time t, $h_j(t)$, equals the sum of the static and dynamic chip thickness: $h_j(t) = h_{j,\mathsf{stat}}(t) + h_{j,\mathsf{dyn}}(t)$.

The cutting force model relates the total chip thickness to the forces acting at the tool tip. The tangential and radial forces, F_t and F_r in Figure 1, for a single tooth j are described by the following exponential cutting force model:

$$\begin{aligned} F_{t_j}(t) &= g_j\big(\phi_j(t)\big) K_t\, a_p\, h_j(t)^{x_F}, \\ F_{r_j}(t) &= g_j\big(\phi_j(t)\big) K_r\, a_p\, h_j(t)^{x_F}, \end{aligned} \tag{1}$$

where $0 < x_F \leq 1$ and $K_t, K_r > 0$ are cutting parameters which depend on the workpiece material. Moreover, a_p is the axial depth of cut. The function $g_j\big(\phi_j(t)\big)$ in (1) describes whether a tooth is in or out of cut:

$$g_j\big(\phi_j(t)\big) = \begin{cases} 1, & \phi_s \leq \phi_j(t) \leq \phi_e \wedge h_j(t) > 0, \\ 0, & \text{else}, \end{cases} \tag{2}$$

where ϕ_s and ϕ_e are the entry and exit angle of the cut, respectively. The total cutting forces in the x- and y-directions, $\underline{F}_t(t) = [F_{t,x}(t)\ F_{t,y}(t)]^T$, can be obtained by summing over all z teeth:

$$\begin{aligned} \underline{F}_t(t) = a_p \sum_{j=0}^{z-1} g_j\big(\phi_j(t)\big) \Big(\Big(h_{j,\mathsf{stat}}(t) \\ + [\sin\phi_j(t)\ \cos\phi_j(t)]\big(\underline{v}_t(t) - \underline{v}_t(t-\tau)\big) \Big)^{x_F} \mathbf{S}_j(t) \begin{bmatrix} K_t \\ K_r \end{bmatrix} \Big) \end{aligned} \tag{3}$$

with

$$\mathbf{S}_j(t) = \begin{bmatrix} -\cos\phi_j(t) & -\sin\phi_j(t) \\ \sin\phi_j(t) & -\cos\phi_j(t) \end{bmatrix}.$$

The cutting force interacts with the machine (spindle and tool) dynamics, which are modeled with a linear multi-input-multi-output (MIMO) state-space model,

$$\begin{aligned} \dot{\underline{x}}(t) &= \mathbf{A}\underline{x}(t) + \mathbf{B}_t \underline{F}_t(t) + \mathbf{B}_a \underline{F}_a(t), \\ \underline{v}_t(t) &= \mathbf{C}_t \underline{x}(t), \quad \underline{v}_a(t) = \mathbf{C}_a \underline{x}(t), \end{aligned} \tag{4}$$

where $\underline{x}(t)$ is the state. $\underline{F}_a(t) = [F_{a,x}(t)\ F_{a,y}(t)]^T$ denote the control forces, where $F_{a,x}(t)$ and $F_{a,y}(t)$ are the control forces acting in the x- and y-direction, respectively.

Substitution of (3) into (4) results in the nonlinear, non-autonomous delay differential equations (DDE) describing the dynamics of the milling process:

$$\begin{aligned} \dot{\underline{x}}(t) &= \mathbf{A}\underline{x}(t) + \mathbf{B}_a \underline{F}_a(t) \\ &\quad + \mathbf{B}_t a_p \sum_{j=0}^{z-1} g_j\big(\phi_j(t)\big) \Big(\Big(h_{j,\mathsf{stat}}(t) \\ &\quad + [\sin\phi_j(t)\ \cos\phi_j(t)] \mathbf{C}_t \big(\underline{x}(t) - \underline{x}(t-\tau)\big) \Big)^{x_F} \mathbf{S}(t) \begin{bmatrix} K_t \\ K_r \end{bmatrix} \Big), \\ \underline{v}_a(t) &= \mathbf{C}_a \underline{x}(t). \end{aligned} \tag{5}$$

The static chip thickness $h_{j,\mathsf{stat}}(t)$ is periodic with period time $\tau = \frac{60}{zn}$. In general, the uncontrolled (i.e. $\underline{F}_a(t) \equiv 0$) milling model (5) has a periodic solution $\underline{x}^*(t)$ with period time τ (Faassen et al., 2007). In the absence of chatter, this periodic solution is (locally) asymptotically stable and when chatter occurs it is unstable. Hence, the chatter stability boundary can be analyzed by studying the (local) stability properties of the periodic solution $\underline{x}^*(t)$. Hereto, the milling model is linearized about the periodic solution $\underline{x}^*(t)$ for zero control input (i.e. $\underline{F}_a(t) \equiv 0$) yielding the following linearized dynamics in terms of perturbations $\underline{\tilde{x}}(t)$ ($\underline{x}(t) = \underline{x}^*(t) + \underline{\tilde{x}}(t)$):

$$\begin{aligned}\dot{\underline{\tilde{x}}}(t) &= \mathbf{A}\underline{\tilde{x}}(t) + a_p\mathbf{B}_t\sum_{j=0}^{z-1}\mathbf{H}_j(\phi_j(t))\mathbf{C}_t(\underline{\tilde{x}}(t) - \underline{\tilde{x}}(t-\tau)) \\ &+ \mathbf{B}_a\underline{F}_a(t), \qquad \underline{\tilde{v}}_a(t) = \mathbf{C}_a\underline{\tilde{x}}(t),\end{aligned} \tag{6}$$

where

$$\mathbf{H}_j(\phi_j(t)) = g_j\big(\phi_j(t)\big)x_F(f_z\sin\phi_j(t))^{x_F-1}\mathbf{S}(t)\begin{bmatrix}K_t\\K_r\end{bmatrix}\begin{bmatrix}\sin\phi_j(t)\\\cos\phi_j(t)\end{bmatrix}^T. \tag{7}$$

The linearized model (6), (7) is a delayed, periodically time-varying system. As described in (Altintas, 2000), for full immersion cuts (studied in this paper) it is sufficient to average the dynamic cutting forces $\sum_{j=0}^{z-1}\mathbf{H}_j(\phi_j(t))$ over the tool path such that the milling model becomes a time-invariant DDE model. Since the cutter is only cutting when $\phi_s \le \phi \le \phi_e$ the averaged cutting forces are given by

$$\bar{\mathbf{H}} = \frac{z}{2\pi}\int_{\phi_s}^{\phi_e}\sum_{j=0}^{z-1}\mathbf{H}_j(\phi)\mathrm{d}\phi. \tag{8}$$

Then, a linear time-invariant model of the milling process is obtained by combining (6) with $\sum_{j=0}^{z-1}\mathbf{H}_j(\phi_j(t)) = \bar{\mathbf{H}}$ and $\bar{\mathbf{H}}$ given in (8).

3. PROBLEM FORMULATION

The objective of this paper is to design a low-order linear controller $\mathbf{K}$ to generate control inputs $\underline{F}_a$ based on measurements $\underline{v}_a$, which guarantees:

- robust stability of $\underline{\tilde{x}} = \underline{0}$ in (6), (7) for 'uncertainties' in depth of cut a_p and time delay τ;
- performance by minimizing the total amount of actuator energy.

By ensuring robust stability for 'uncertainties' in a_p and τ, chatter-free milling operations can be guaranteed in an a priori defined range of spindle speeds $n = \frac{60}{z\tau}$ and depth of cut a_p. Moreover, we will include the limitation of the actuator forces as a performance criterion in the controller design since it is also an important practical performance specification. An important aspect in the development of an active chatter control design strategy is the selection of the variable used for feedback (van Dijk et al., 2011a). In particular, it is concluded that perturbation feedback (i.e. using $\underline{\tilde{v}}_a$ as an input to the controller) is beneficial for reducing required actuator forces without compromising performance (in terms of the achievable closed-loop depth of cut/spindle speed interval for which chatter can be eliminated). Here, we introduce dynamic *Pyragas-type delayed* output feedback for robust stabilization of the high-speed milling process to implement such perturbation feedback.

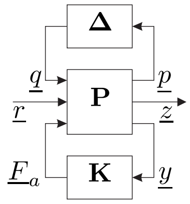

Fig. 2. Generalized plant interconnection.

The proposed (Pyragas-type) controller $\mathbf{K}$, with input $\underline{\tilde{v}}_a \in \mathbb{R}^2$ and output (control action) $\underline{F}_a \in \mathbb{R}^2$, has the following state-space description:

$$\begin{aligned}\dot{\underline{\xi}}(t) &= \mathbf{A}_c\underline{\xi}(t) + \mathbf{B}_c(\underline{\tilde{v}}_a(t) - \underline{\tilde{v}}_a(t-\tau)),\\ \underline{F}_a(t) &= \mathbf{C}_c\underline{\xi}(t) + \mathbf{D}_c(\underline{\tilde{v}}_a(t) - \underline{\tilde{v}}_a(t-\tau)).\end{aligned} \tag{9}$$

Herein, $\underline{\xi} \in \mathbb{R}^{n_c}$, $\mathbf{A}_c \in \mathbb{R}^{n_c\times n_c}$, $\mathbf{B}_c \in \mathbb{R}^{n_c\times 2}$, $\mathbf{C}_c \in \mathbb{R}^{2\times n_c}$ and $\mathbf{D_c} \in \mathbb{R}^{2\times 2}$ with n_c the order of the controller. The benefit of employing Pyragas-type feedback control lies in the fact that the signal $\underline{\tilde{v}}_a(t)$ can typically not be measured directly. By realizing that $\underline{\tilde{v}}_a(t) - \underline{\tilde{v}}_a(t-\tau) = \underline{v}_a(t) - \underline{v}_a(t-\tau)$, since $\underline{v}_a^*(t) = \underline{v}_a^*(t-\tau)$ (with $\underline{v}_a^* = \mathbf{C}_a\underline{x}^*$) holds due to the periodic nature of the chatter-free solution, the controller in (9) can be directly implemented using only measurement of $\underline{v}_a(t)$ (without the need for online estimation algorithms to estimate the chatter vibrations $\underline{\tilde{v}}_a(t)$).

4. GENERALIZED PLANT FORMULATION

To solve the problem formulated in Section 3, the milling model will be extended with uncertainties in depth of cut a_p and spindle speed n. For this purpose, the control goal will be cast into the generalized plant framework, see Figure 2. The generalized plant $\mathbf{P}$ is a given system with three sets of inputs and three sets of outputs. The signal pair $\underline{p}, \underline{q}$ denote the in-/outputs of the uncertainty channel connecting the plant to the uncertainty block $\mathbf{\Delta}$. The signal $\underline{r}$ represents an external input in which possible disturbances, measurement noise and reference inputs are stacked. The signal $\underline{F}_a$ is the control input. The output $\underline{z}$ can be considered as a performance variable while $\underline{y}(t) = \mathbf{C}_a(\underline{\tilde{x}}(t) - \underline{\tilde{x}}(t-\tau)) = \underline{\tilde{v}}_a(t) - \underline{\tilde{v}}_a(t-\tau)$ denotes the outputs used for feedback.

To construct the generalized plant formulation, consider the linear time-invariant model of the milling process, obtained by combining (6) with $\sum_{j=0}^{z-1}\mathbf{H}_j(\phi_j(t)) = \bar{\mathbf{H}}$ and $\bar{\mathbf{H}}$ given in (8). Let us define the following uncertainty sets:

$$a_p = \tfrac{1}{2}\bar{a}_p(1 + \delta_{a_p}) \text{ and } \tau = \tau_0 + \delta_\tau, \tag{10}$$

where $\bar{a}_p$ is the maximal depth of cut for which stable milling is desired, $\delta_{a_p} \in \mathbb{C}$, $|\delta_{a_p}| \le 1$, $\tau_0 = \frac{\bar{\tau}+\underline{\tau}}{2}$ and $\delta_\tau \in \frac{\bar{\tau}-\underline{\tau}}{2}[-1, 1]$, such that $0 < \underline{\tau} < \bar{\tau}$. Here, $\underline{\tau}$ and $\bar{\tau}$ together define the range of spindle speeds $\left[\frac{60}{z\bar{\tau}}, \frac{60}{z\underline{\tau}}\right]$ for which stable milling is desired. Moreover, as motivated in Section 3, it is desired to limit the magnitude of the actuator forces.

Therefore, the performance output $\underline{z}$ is chosen as the weighted control input $\underline{z}(s) = \mathbf{W}_{KS}(s)\underline{F}_a(s)$, $s \in \mathbb{C}$, where $\mathbf{W}_{KS}$ is a stable weighting filter with the following state-space realization:

$$\begin{aligned} \dot{\underline{x}}_{KS}(t) &= \mathbf{A}_{KS}\underline{x}_{KS}(t) + \mathbf{B}_{KS}\underline{F}_a(t), \\ \underline{z}(t) &= \mathbf{C}_{KS}\underline{x}_{KS}(t) + \mathbf{D}_{KS}\underline{F}_a(t). \end{aligned} \tag{11}$$

Substituting (10) in (6) with $\sum_{j=0}^{z-1}\mathbf{H}_j(\phi_j(t)) = \bar{\mathbf{H}}$ and $\bar{\mathbf{H}}$ given in (8) and by adding the performance in-/output channels to the system (and rearranging terms), the state-space representation of the generalized plant $\mathbf{P}$ is given by:

$$\begin{aligned} \dot{\underline{x}}_P(t) &= \mathbf{A}_{P,0}\underline{x}_P(t) + \mathbf{A}_{P,1}\underline{x}_P(t-\tau_0) + \mathbf{B}_P\underline{u}_P(t) \\ \underline{v}_P(t) &= \mathbf{C}_{P,0}\underline{x}_P(t) + \mathbf{C}_{P,1}\underline{x}_P(t-\tau_0) + \mathbf{D}_P\underline{u}_P(t) \end{aligned} \tag{12}$$

with the state vector $\underline{x}_P(t) = [\tilde{\underline{x}}^T(t)\ \underline{x}_{KS}^T(t)]^T$, input vector $\underline{u}_P(t) = [\underline{q}^T(t)\ \underline{r}^T(t)\ \underline{F}_a^T(t)]^T$, with $\underline{r} \in \mathbb{R}^2$ representing measurement noise on the output $\underline{y}$, and output vector $\underline{v}_P(t) = [\underline{p}^T(t)\ \underline{z}^T(t)\ \underline{y}^T(t)]^T$. The (structured) uncertainty channel input $\underline{p}(t)$ and output $\underline{q}(t)$ are defined as

$$\underline{p}(t) = \begin{bmatrix} \underline{p}_1(t) \\ \underline{p}_2(t) \\ \underline{p}_3(t) \end{bmatrix} := \begin{bmatrix} \mathbf{C}_t\underline{x}(t-\tau_0) \\ \mathbf{C}_a\underline{x}(t-\tau_0) \\ \frac{1}{2}\bar{a}_p\mathbf{C}_t(\underline{x}(t) - \underline{x}(t-\tau_0)) - \frac{1}{2}\bar{a}_p q_1(t) \end{bmatrix}, \tag{13}$$

$$\underline{q}(t) = \begin{bmatrix} \underline{q}_1(t) \\ \underline{q}_2(t) \\ \underline{q}_3(t) \end{bmatrix} := \begin{bmatrix} (\mathcal{D}_{\delta_\tau} - 1)\underline{p}_1(t) \\ (\mathcal{D}_{\delta_\tau} - 1)\underline{p}_2(t) \\ \delta a_p \underline{p}_3(t) \end{bmatrix}, \tag{14}$$

where the delay-operator $\mathcal{D}_{\delta_\tau}$ is defined as $\mathcal{D}_{\delta_\tau}\underline{x}(t) = \underline{x}(t-\delta_\tau)$. The state-space matrices of the generalized plant in (12) are given by

$$\mathbf{A}_{P,0} = \begin{bmatrix} \mathbf{A} + \frac{1}{2}\bar{a}_p\mathbf{B}_t\bar{\mathbf{H}}\mathbf{C}_t & \mathbf{0} \\ \mathbf{0} & \mathbf{A}_{KS} \end{bmatrix},\ \mathbf{A}_{P,1} = \begin{bmatrix} -\frac{1}{2}\bar{a}_p\mathbf{B}_t\bar{\mathbf{H}}\mathbf{C}_t & \mathbf{0} \\ \mathbf{0} & \mathbf{0} \end{bmatrix},$$

$$\mathbf{B}_P = \left[\begin{array}{ccc|cc} -\frac{1}{2}\bar{a}_p\mathbf{B}_t\bar{\mathbf{H}} & \mathbf{0} & \mathbf{B}_t\bar{\mathbf{H}} & \mathbf{0} & \mathbf{B}_a \\ \mathbf{0} & \mathbf{0} & \mathbf{0} & \mathbf{0} & \mathbf{B}_{KS} \end{array}\right],$$

$$\mathbf{C}_{P,0} = \left[\begin{array}{cc} \mathbf{0} & \mathbf{0} \\ \mathbf{0} & \mathbf{0} \\ \frac{1}{2}\bar{a}_p\mathbf{C}_t & \mathbf{0} \\ \hline \mathbf{0} & \mathbf{C}_{KS} \\ \mathbf{C}_a & \mathbf{0} \end{array}\right],\ \mathbf{C}_{P,1} = \left[\begin{array}{cc} \mathbf{C}_t & \mathbf{0} \\ \mathbf{C}_a & \mathbf{0} \\ -\frac{1}{2}\bar{a}_p\mathbf{C}_t & \mathbf{0} \\ \hline \mathbf{0} & \mathbf{0} \\ -\mathbf{C}_a & \mathbf{0} \end{array}\right],$$

$$\mathbf{D}_P = \left[\begin{array}{ccc|cc} \mathbf{0} & \mathbf{0} & \mathbf{0} & \mathbf{0} & \mathbf{0} \\ \mathbf{0} & \mathbf{0} & \mathbf{0} & \mathbf{0} & \mathbf{0} \\ -\frac{1}{2}\bar{a}_p\mathbf{I}_2 & \mathbf{0} & \mathbf{0} & \mathbf{0} & \mathbf{0} \\ \hline \mathbf{0} & \mathbf{0} & \mathbf{0} & \mathbf{0} & \mathbf{D}_{KS} \\ \mathbf{0} & -\mathbf{I}_2 & \mathbf{0} & \mathbf{I}_2 & \mathbf{0} \end{array}\right]$$

with identity matrix $\mathbf{I}_n \in \mathbb{R}^{n\times n}$.

The transfer function description of the generalized plant $\mathbf{P}$ is given by:

$$\mathbf{P}(s) = \left(\mathbf{C}_{P,0} + \mathbf{C}_{P,1}e^{-s\tau_0}\right)\left[s\mathbf{I} - \mathbf{A}_{P,0}\right. \tag{15}$$

$$\left. - \mathbf{A}_{P,1}e^{-s\tau_0}\right]^{-1}\mathbf{B}_P + \mathbf{D}_P, \tag{16}$$

where $s \in \mathbb{C}$. By $\mathbf{\Delta}(s)$ we denote the Laplace transform of the uncertainty term (14), such that $\underline{q}(s) = \mathbf{\Delta}(s)\underline{p}(s)$ with

$$\mathbf{\Delta}(s) = \begin{bmatrix} (e^{-s\delta_\tau} - 1)\mathbf{I}_4 & \mathbf{0} \\ \mathbf{0} & \delta_{a_p}\mathbf{I}_2 \end{bmatrix}. \tag{17}$$

The uncertainty term Δ depends on the frequency. The delay uncertainty $e^{-s\delta_\tau} - 1$ can be upper bounded by a (non-rational) frequency-dependent upper bound $\kappa(\omega)$ as follows (Huang and Zhou, 2000):

$$\kappa(\omega) = \begin{cases} 2\sin\dfrac{\delta_\tau\omega}{2}, & \forall\omega,\ 0 \le \omega \le \pi/\delta_\tau \\ 2, & \forall\omega \ge \pi/\delta_\tau, \end{cases} \tag{18}$$

in the sense that $|e^{-i\omega\delta_\tau} - 1| \le \kappa(\omega)$. By defining $\mathbf{L}(s) = \mathrm{diag}(\kappa(\omega)\mathbf{I}_4, \mathbf{I}_2)$, for all $s = \xi + i\omega$, with $\xi,\ \omega \in \mathbb{R}$, the (scaled) generalized plant and uncertainty term can be written as follows:

$$\tilde{\mathbf{P}}(s) = \mathrm{diag}(\mathbf{L}(s), \mathbf{I}_2, \mathbf{I}_2)\mathbf{P}(s),\ \tilde{\mathbf{\Delta}} = \mathbf{\Delta}(s)\mathbf{L}^{-1}(s). \tag{19}$$

5. SYNTHESIS OF LOW-ORDER PYRAGAS-TYPE FEEDBACK CONTROLLERS

Based on the above clarifies that the design of a controller guaranteeing robustness properties with respect to the (scaled) uncertainty $\tilde{\mathbf{\Delta}}$ requires the solution of the following optimization problem:

$$\begin{aligned} &\min_{\mathbf{K}}\sup_{\omega\in\mathbb{R}} \mu_{\tilde{\mathbf{\Delta}}}(\mathbf{N}), \\ &\text{subject to } \Psi(\mathbf{K}) < 0, \end{aligned} \tag{20}$$

with $\mathbf{N}$ the lower fractional transformation (LFT) of $\tilde{\mathbf{P}}$ in (19) and fixed-structure controller $\mathbf{K}$ in (9) and $\Psi(\mathbf{K})$ the spectral abscissa function of the closed-loop system defined as:

$$\Psi(\mathbf{K}) := \sup\{\Re(\lambda) : \det(\lambda\mathbf{I} - \bar{\mathbf{A}}_0 - \bar{\mathbf{A}}_1 e^{-\lambda\tau_0}) = 0\}, \tag{21}$$

where

$$\bar{\mathbf{A}}_0 = \begin{bmatrix} \mathbf{A} + \frac{1}{2}\bar{a}_p\mathbf{B}_t\bar{\mathbf{H}}\mathbf{C}_t & \mathbf{0} \\ \mathbf{0} & \mathbf{0} \end{bmatrix} + \begin{bmatrix} \mathbf{B}_a & \mathbf{0} \\ \mathbf{0} & \mathbf{I} \end{bmatrix}\begin{bmatrix} \mathbf{D}_c & \mathbf{C}_c \\ \mathbf{B}_c & \mathbf{A}_c \end{bmatrix}\begin{bmatrix} \mathbf{C}_a & \mathbf{0} \\ \mathbf{0} & \mathbf{I} \end{bmatrix},$$

$$\bar{\mathbf{A}}_1 = \begin{bmatrix} -\frac{1}{2}\bar{a}_p\mathbf{B}_t\bar{\mathbf{H}}\mathbf{C}_t & \mathbf{0} \\ \mathbf{0} & \mathbf{0} \end{bmatrix} + \begin{bmatrix} \mathbf{B}_a & \mathbf{0} \\ \mathbf{0} & \mathbf{I} \end{bmatrix}\begin{bmatrix} \mathbf{D}_c & \mathbf{C}_c \\ \mathbf{B}_c & \mathbf{A}_c \end{bmatrix}\begin{bmatrix} -\mathbf{C}_a & \mathbf{0} \\ \mathbf{0} & \mathbf{0} \end{bmatrix}.$$

The constraint on the objective function, defined above, is a necessary condition to guarantee the existence of the $\mathcal{H}_\infty$-norm of $\mathbf{N}$ along with stability of the closed-loop system (Zhou et al., 1996).

The robust stability and performance requirement can now be translated into the demand that the objective function in (20) is smaller than one. It is in general hard to calculate $\mu_{\tilde{\mathbf{\Delta}}}(\mathbf{N})$. Nevertheless, an upper bound on $\mu_{\tilde{\mathbf{\Delta}}}(\mathbf{N})$ can be obtained by calculating the scaled $\mathcal{H}_\infty$ norm of $\mathbf{N}$ (Zhou et al., 1996). Since the uncertainties are modeled as complex uncertainties, see (10) and (17), D-K-iteration, see (Zhou et al., 1996), pro ides a reasonable approach towards solving the problem. Hereby, the optimization problem is described by:

$$\begin{aligned} &\min_{\mathbf{K}}\inf_{\mathbf{D}\in\boldsymbol{\mathcal{H}}_\infty} \|\mathbf{D}\mathbf{N}\mathbf{D}^{-1}\|_\infty, \\ &\text{subject to } \Psi(\mathbf{K}) < 0, \end{aligned} \tag{22}$$

which is iteratively solved for $\mathbf{K}$ and $\mathbf{D}$. Herein,

$$\|\mathbf{D}\mathbf{N}\mathbf{D}^{-1}\|_\infty = \sup_{\omega\in\mathbb{R}} \bar{\sigma}\left(\mathbf{D}(i\omega)\mathbf{N}(i\omega)\mathbf{D}(i\omega)^{-1}\right),$$

$\boldsymbol{\mathcal{H}}_\infty$ denotes the set of functions that are analytic and bounded in the open right half plane, and the structure of $\mathbf{D}$ is chosen such that $\mathbf{D}$ commutes with the uncertainty set $\tilde{\mathbf{\Delta}}$, i.e. satisfies $\mathbf{D}\tilde{\mathbf{\Delta}} = \tilde{\mathbf{\Delta}}\mathbf{D}$. For more details on the computation of lower and upper bounds on the complex structured singular value, we refer to (Packard and Doyle, 1993). For a given $\mathbf{K}$, the problem of finding the scaling matrix $\mathbf{D}$ can be formulated as a convex optimization problem which is generally solved pointwise in the frequency domain (for example, by using the `mussv` command

Table 1. Milling model parameters.

Parameter	Value	Parameter	Value
$m_{t,x} = m_{t,y}$	0.015 kg	K_t	462 [N/mm$^{(1+x_F)}$]
$m_{a,x} = m_{a,y}$	0.14 kg	K_r	38.6 [N/mm$^{(1+x_F)}$]
$\omega_{t,x} = \omega_{t,y}$	2350 Hz	z	4 [-]
$\omega_{a,x} = \omega_{a,y}$	1400 Hz	ϕ_s	0 [rad]
$\zeta_{t,x} = \zeta_{t,y}$	0.05 [-]	ϕ_e	π [rad]
$\zeta_{a,x} = \zeta_{a,y}$	0.12 [-]	f_z	0.2 mm/tooth

from the Robust Control Toolbox of MATLAB. Given our goal of designing fixed-structure controllers, the problem of finding $\mathbf{K}$, for a given $\mathbf{D}$, in general results in the following non-convex, non-smooth, constrained optimization problem:

$$\min_{\mathbf{K}} f(\mathbf{K}), \text{ subject to } \Psi(\mathbf{K}) < 0 \tag{23}$$

with $f(\mathbf{K}) := \sup_{\omega\in\mathbb{R}} \bar{\sigma}\big(\mathbf{D}(i\omega)\mathbf{N}(i\omega)\mathbf{D}(i\omega)^{-1}\big)$.

The non-smooth dependency of the objective function (23) on the controller parameters of $\mathbf{K}$ typically occurs when the maximum of the objective function is located at two (or more) different frequencies. Due to the non-smoothness in (23), standard optimization algorithms cannot be used to determine the (optimal) parameters of controller $\mathbf{K}$. Instead, we employ a non-smooth optimization technique, namely a gradient bundle method called gradient sampling developed in (Burke et al., 2005).

For further details on the optimization-based algorithm (and the role of gradient sampling herein) used to solve the above fixed-structure robust controller synthesis problem and other fixed-order control designs than those based on Pyragas-type feedback, we refer to (van Dijk, 2011; van Dijk et al., 2015).

6. CONTROLLER SYNTHESIS RESULTS

This section presents the results of the application of the controller synthesis methodology, presented in Section 5, to the robust chatter control problem.

Here, the machine spindle-toolholder-tool dynamics in (4) is modeled by two decoupled subsystems (representing the dynamics in two (x,y) orthogonal directions perpendicular to the spindle axis). The dynamics in both the x- and y-directions are modeled as two-degree-of-freedom mass-spring-damper systems with masses $m_{i,k}$, $i \in \{a,t\}$, $k \in \{x,y\}$, with $m_{t,x}$, $m_{t,y}$ the tool mass in x-, y-direction and $m_{a,x}$, $m_{a,y}$ the spindle/actuator mass in x-, y-direction, the eigenfrequencies $\omega_{i,k} = \sqrt{(c_{i,k}/m_{i,k})}$, $i \in \{a,t\}$, $k \in \{x,y\}$, and dimensionless damping ratios $\zeta_{i,k} = b_{i,k}/2\sqrt{(c_{i,k}m_{i,k})}$, $i \in \{a,t\}$, $k \in \{x,y\}$. This model is adopted to capture the inherent dynamics between the actuator/sensor system (denoted by subscript a) and the cutting tool (denoted by subscript t). The parameters of the milling model are given in Table 1. Moreover, $x_F = 0.744$, reflecting a nonlinear cutting model. Next, the results of synthesizing dynamic Pyragas-type delayed output controllers as defined by (9) are presented.

The Pyragas-type dynamic output feedback controller will be designed such that milling operations between $n \in [34000, 36000]$ rpm are stabilized, for a depth of cut which is as large as possible given the performance requirement

Table 2. Results from fixed-structure controller synthesis for three different controller orders.

n_c [-]	No. D-K-steps	$\mu_{\hat{\Delta}}$ [-]	$\bar{a}_p$ [mm]	$a_{p,\max}$
0	7	0.9983	1.1250	1.4690
2	10	0.9918	1.8250	2.1456
4	9	0.9810	2.0000	2.3992

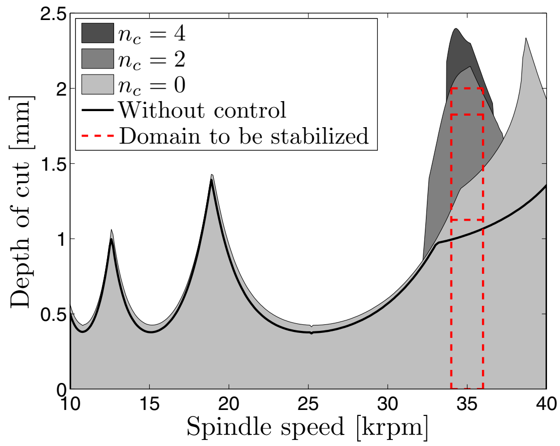

Fig. 3. Stability lobes diagram for controllers of order $n_c = 0, 2$ and 4, respectively, and without control. The area for which robust stability is guaranteed is indicated by the dashed boxes, see also Table 2.

on the weighted control sensitivity. Here, the performance weighting W_{KS} is chosen as

$$W_{KS}(s) = K_p \frac{\frac{1}{2\pi f_{r,l}}s+1}{\frac{1}{2\pi f_{p,l}}s+1} \cdot \frac{\frac{1}{2\pi f_{r,h}}s+1}{\frac{1}{2\pi f_{p,h}}s+1}, \tag{24}$$

with $K_p = 1 \cdot 10^{-6}$ mm/N, $f_{r,l} = 100$ Hz, $f_{r,h} = 7500$ Hz, $f_{p,l} = 1 \cdot 10^{-2}$ Hz and $f_{p,h} = 2 \cdot 10^4$ Hz.

Three low-order Pyragas-type controllers are synthesized, namely for $n_c = 0$ (i.e. static delayed output feedback), and $n_c = 2$ and $n_c = 4$ (i.e. dynamic delayed output feedback), using the algorithm as presented in Section 5. The results are listed in Table 2. Herein, $\bar{a}_p$ denotes the maximal depth of cut for which robust performance can be guaranteed and $a_{p,\max}$ denotes the maximal depth of cut in the Stability Lobes Diagram (SLD) for the desired spindle speed interval. The resulting controllers are given in Figure 4. This figure shows that the controllers designed for $n_c = 2$ and $n_c = 4$ are dynamic MIMO controllers with notch characteristics. The SLDs are computed using the semi-discretization method (Insperger and Stépán, 2004) with the designed controllers and without control using the linearized time-variant model of the milling process in (6). The corresponding results are given in Figure 3. From the figure, it can be observed that for the case where $n_c = 0$ the fixed-structure controller indeed alters the SLD. In this case, based on the SLD, the depth of cut can be increased from $a_{p,\max} = 1.067$ mm in open loop to 1.469 mm in closed loop, which is an improvement of approximately 38%. The peak of the closed-loop stability lobe is approximately located at $n = 38700$ rpm, which is outside the domain of desired spindle speeds. Of course, if the peak of the SLD could be placed inside the desired interval of spindle speeds, then a higher maximum depth of cut could be achieved. In order to shift the peak of the lobe at such a spindle speed, the controller, in this case, needs

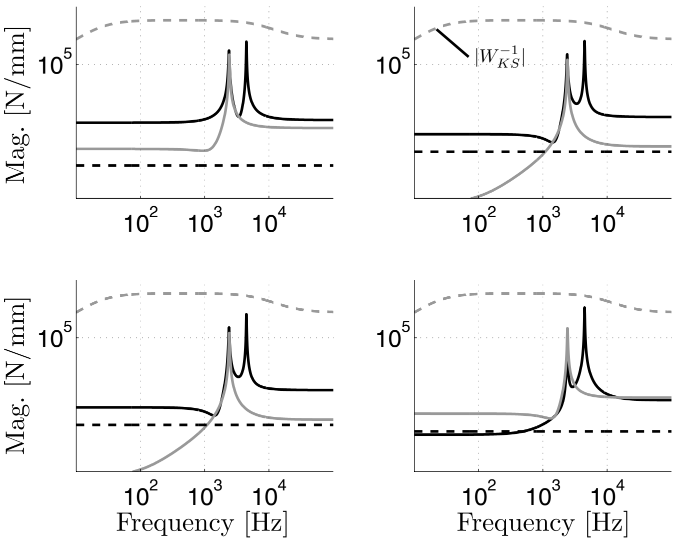

Fig. 4. Magnitude of the fixed-structure controllers of order $n_c = 0$ (black dashed), $n_c = 2$ (grey solid) and $n_c = 4$ (black solid). Also the magnitude of the inverse of the performance weighting function W_{KS} is given.

to exhibit more complex dynamics, which is obtained by increasing the controller order.

For the dynamic fixed-structure controllers with $n_c = 2$ and $n_c = 4$ it can be observed in Figure 3 that the SLD is altered such that a lobe is indeed created at the desired spindle speed interval. Clearly, by increasing the order of the fixed-structure controller, the area for which robust stability is guaranteed is increased. In this case, based on the SLD in Figure 3, the depth of cut can be increased from $a_{p,\max} = 1.067$ mm to $a_{p,\max} = 2.146$ for $n_c = 2$ and to $a_{p,\max} = 2.399$ for $n_c = 4$, which leads to a productivity increase of approximately 101% and 125%, respectively. Figure 3 clearly illustrates the benefit of dynamic controllers over the static controllers proposed in (van Dijk et al., 2011b).

7. CONCLUSION

This paper presents a strategy for the design of low-order controllers guaranteeing robust stability and performance of the high-speed milling process; in particular, the avoidance of chatter in a predefined area of depth-of-cut and spindle speed while respecting limitations regarding the required actuator forces.

We have proposed Pyragas-type delayed dynamic output-feedback controllers, thereby simplifying their implementation in practice as no additional estimators for chatter-related vibrations are needed. Moreover, the approach enables the design of relatively low-order controllers, which is desirable from a real-time implementation perspective especially given the high-frequency characteristics of the milling dynamics. The presented example illustrates the merit of the proposed controller synthesis strategy in terms of ensuring a significantly higher material removal rate in closed loop while avoiding chatter.

REFERENCES

Altintas, Y. (2000). *Manufacturing automation*. Cambridge University Press, Cambridge, UK.

Burke, J., Lewis, A., and Overton, M. (2005). A robust gradient sampling algorithm for nonsmooth, nonconvex optimization. *SIAM Journal on Optimization*, 15(3), 751–779.

Chen, M. and Knospe, C.R. (2007). Control approaches to the suppression of machining chatter using active magnetic bearings. *IEEE Trans. on Control Systems Technology*, 15(2), 220–232.

Dohner, J.L., Lauffer, J.P., Hinnerichs, T.D., Shankar, N., Regelbrugge, M.E., Kwan, C.M., Xu, R., Winterbauer, B., and Bridger, K. (2004). Mitigation of chatter instabilities in milling by active structural control. *Journal of Sound and Vibration*, 269(1-2), 197–211.

Faassen, R.P.H., van de Wouw, N., Nijmeijer, H., and Oosterling, J.A.J. (2007). An improved tool path model including periodic delay for chatter prediction in milling. *Journal of Computational and Nonlinear Dynamics*, 2(2), 167–179.

Faassen, R.P.H., van de Wouw, N., Oosterling, J.A.J., and Nijmeijer, H. (2003). Prediction of regenerative chatter by modelling and analysis of high-speed milling. *International Journal of Machine Tools and Manufacture*, 43(14), 1437–1446.

Huang, Y.P. and Zhou, K. (2000). Robust stability of uncertain time-delay systems. *IEEE Transactions on Automatic Control*, 45(11), 2169–2173.

Insperger, T. and Stépán, G. (2004). Updated semi-discretization method for periodic delay-differential equations with discrete delay. *International Journal for Numerical Methods in Engineering*, 61(1), 117–141.

Insperger, T., Stépán, G., Bayly, P.V., and Mann, B.P. (2003). Multiple chatter frequencies in milling processes. *Journal of Sound and Vibration*, 262(2), 333–345.

Kern, S., Ehmann, C., Nordmann, R., Roth, M., Schiffler, A., and Abele, E. (2006). Active damping of chatter vibrations with an active magnetic bearing in a motor spindle using μ-synthesis and an adaptive filter. In *The 8th International Conference on Motion and Vibration Control*.

Packard, A. and Doyle, J. (1993). The complex structured singular value. *Automatica*, 29(1), 71–109.

Pyragas, K. (1992). Continuous control of chaos by self-controlling feedback. *Physics Letters A*, 170(6), 421–428.

Shiraishi, M., Yamanaka, K., and Fujita, H. (1991). Optimal control of chatter in turning. *International Journal of Machine Tools and Manufacture*, 31(1), 31–43.

Stépán, G. (2001). Modelling nonlinear regenerative effects in metal cutting. *Philosophical transactions of the royal society A: mathematical, physical and engineering sciences*, 359(1781), 739–757. doi:10.1098/rsta.2000.0753.

van Dijk, N.J.M., Doppenberg, E.J.J., Faassen, R.P.H., van de Wouw, N., Oosterling, J.A.J., and Nijmeijer, H. (2010). Automatic in-process chatter avoidance in the high-speed milling process. *Journal of Dynamic systems, Measurement and Control*, 132(3), 031006 (14 pages).

van Dijk, N.J.M., van de Wouw, N., Doppenberg, E.J.J., Oosterling, J.A.J., and Nijmeijer, H. (2011a). Robust active chatter control in the high-speed milling process. *IEEE Transactions on Control Systems Technology*, 20(4), 901–917.

van Dijk, N.J.M., van de Wouw, N., and Nijmeijer, H. (2011b). Low-order control design for chatter suppression in high-speed milling. In *Proceedings of the Conference on Decision and Control*, 663–668. Orlando, FL, USA.

van Dijk, N.J.M., van de Wouw, N., and Nijmeijer, H. (2015). Fixed-structure robust controller design for chatter mitigation in high-speed milling. *International Journal of Robust and Nonlinear Control*. Submitted.

van Dijk, N. (2011). *Active chatter control in high-speed milling processes*. Ph.D. thesis, Eindhoven University of Technology. Http://www.dct.tue.nl/New/Wouw/phdthesisvandijk2011.pdf.

Zhang, Y. and Sims, N.D. (2005). Milling workpiece chatter avoidance using piezoelectric active damping: A feasibility study. *Smart materials and structures*, 14(6), N65–N70.

Zhou, K., Doyle, J.C., and Glover, K. (1996). *Robust and Optimal Control*. Prentice Hall, Upper Saddle River, USA.